

Multiplicatively Repeated Non-Binary LDPC Codes

Kenta Kasai, David Declercq, Charly Poulliat, *Member, IEEE*, and Kohichi Sakaniwa, *Senior Member, IEEE*

Abstract—We propose non-binary LDPC codes concatenated with multiplicative repetition codes. By multiplicatively repeating the (2,3)-regular non-binary LDPC mother code of rate $1/3$, we construct rate-compatible codes of lower rates $1/6, 1/9, 1/12, \dots$. Surprisingly, such simple low-rate non-binary LDPC codes outperform the best low-rate binary LDPC codes so far. Moreover, we propose the decoding algorithm for the proposed codes, which can be decoded with almost the same computational complexity as that of the mother code.

Index Terms—iterative decoding, low-rate code, non-binary low-density parity-check code, rate compatible code, repetition code

I. INTRODUCTION

In 1963, Gallager invented low-density parity-check (LDPC) codes [2]. Due to sparsity of the code representation, LDPC codes are efficiently decoded by belief propagation (BP) decoders. By a powerful optimization method *density evolution* [3], developed by Richardson and Urbanke, messages of BP decoding can be statistically evaluated. The optimized LDPC codes can approach very close to Shannon limit [4].

Rate-adaptability is a desirable property of coding systems. Over time-varying channels, the system adapts the coding rate according to the quality of the channels. Using the different type of codes for different rates results in a complex coding system. It is desirable to use a single encoder and decoder pair compatible with different rates. Such a property of codes is referred to as rate-compatibility. Moreover, rate-compatible codes allow us to transmit bits gradually in conjunction with automatic repeat request (ARQ). By puncturing a low rate code, we can construct rate-compatible codes of higher rates.

In order to reliably transmit information over the very noisy communication channels, one needs to encode the information at low coding rate. As described in [5], one encounters a difficulty when designing low-rate LDPC codes. While, for high rate codes, even binary regular LDPC codes have good thresholds. The optimized low-rate structured LDPC codes, e.g. accumulate repeat accumulate (ARA) code [6, Table. 1] of rate $1/6$ and multi-edge type LDPC code [5, Table. X] of rate $1/10$ have good thresholds. However, the maximum row-weights of those codes are as high as 11 and 28, respectively. Such high row weights lead to dense parity-check matrices and degraded performance for short code length. We note that, with very large code length, generalized LDPC codes

with Hadamard codes [7] perform very close to the ultimate Shannon limit [8]. However, the large code length leads to transmission latency. If two error correcting codes with the same error-correcting capabilities and different code length are given, the shorter code is preferred.

Another obstacle blocking the realization of the low-rate LDPC codes is the large number of check node computations. For a fixed information length K , it can be easily seen that the number M of check nodes gets larger as the coding rate R gets lower. To be precise, $M = K(1 - R)/R$. In the BP decoding, computations of check nodes are usually more complex than those of variable nodes. It is a desirable property for the low-rate LDPC codes to be decoded with computational complexity comparable to that of the higher-rate LDPC codes.

The problems for constructing low-rate LDPC codes are summarized as follows.

- **Problem 1:** The Tanner graphs of low-rate LDPC codes tend to have many check nodes that require more complex computations than variable nodes.
- **Problem 2:** The Tanner graphs of optimized low-rate LDPC codes tend to have check nodes of high degree, which results in the degraded decoding performance for small code length.
- **Problem 3:** The optimized low-rate LDPC codes need to be used with large code length to exploit the potential decoding performance.

In this paper, we deal with all these issues.

In this paper, we consider non-binary LDPC codes defined by sparse parity-check matrices over $\text{GF}(2^m)$ for $2^m > 2$. Non-binary LDPC codes were invented by Gallager [2]. Davey and MacKay [9] found non-binary LDPC codes can outperform binary ones. Non-binary LDPC codes have captured much attention recently due to their decoding performance [10], [11], [12], [13], [14].

It is known that irregularity of Tanner graphs help improve the decoding performance of binary LDPC codes [4]. While, it is not the case for the non-binary LDPC codes. The $(2, k)$ -regular non-binary LDPC codes over $\text{GF}(2^m)$ are empirically known [15] as the best performing codes for $2^m \geq 64$, especially for short code length. This means that, for designing non-binary LDPC codes, one does not need to optimize the degree distributions of Tanner graphs, since $(2, k)$ -regular non-binary LDPC codes are best. Furthermore, sparsity of $(2, k)$ -regular Tanner graph helps efficient decoding.

Sassatelli et al. proposed *hybrid non-binary LDPC codes* [16] whose symbols are defined over the Galois fields of different sizes, e.g. over $\text{GF}(2)$, $\text{GF}(8)$, and $\text{GF}(16)$ and whose Tanner graphs are irregular. In other words, the codes have two types of irregularity, i.e. irregularity of the degree distributions of graphs and the size distributions of Galois fields. To the best of the authors' knowledge, the decoding

The material in this paper was presented in part at 2010 IEEE International Symposium on Information Theory (ISIT) [1].

K. Kasai and K. Sakaniwa are with the Department of Communications and Integrated Systems, Graduate School of Science and Engineering, Tokyo Institute of Technology, 2-12-1 Ookayama, Meguro-ku, Tokyo 152-8550, Japan (e-mail: {kenta, sakaniwa}@comm.ss.titech.ac.jp).

D. Declercq and C. Poulliat are with the ETIS Laboratory, UMR8051 ENSEA UCP CNRS, 95014 Cergy-Pontoise, France (e-mail: {declercq, poulliat}@ensea.fr).

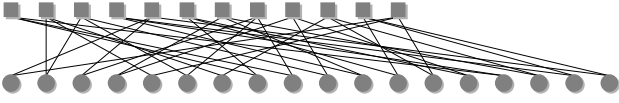


Fig. 1. An example of a mother code C_1 . A non-binary (2,3)-regular LDPC code of rate $1/3$ over $\text{GF}(2^m)$. Each variable node represents a symbol in $\text{GF}(2^m)$. Each check node represents a parity-check equation over $\text{GF}(2^m)$. The code length is 18 symbols in $\text{GF}(2^m)$ or equivalently $18m$ bits. Circle and square nodes represent variable and check nodes, respectively. The lower-rate codes C_T for $T = 2, 3, \dots$ are constructed from C_1 .

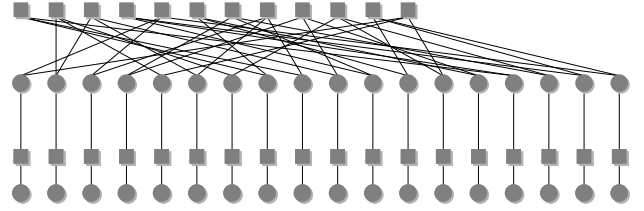


Fig. 2. An example of C_2 . A non-binary (2,3)-regular LDPC code over $\text{GF}(2^m)$ concatenated with inner multiplicative repetition codes of length 2. The code length is 36 symbols or equivalently $36m$ bits. The rate is $1/6$.

performance of the hybrid non-binary LDPC codes are best so far among the low-rate codes of short code length.

In this paper, we investigate non-binary LDPC codes concatenated with multiplicative repetition inner codes. We use a (2, 3)-regular non-binary LDPC code of rate $1/3$, as a mother code. By multiplicatively repeating the mother code, we construct codes of lower rates $1/6, 1/9, 1/12, \dots$. Furthermore, we present a decoding algorithm for the proposed codes. And we show the computational complexity of decoding is almost the same as that of the mother code. The codes exhibit surprisingly better decoding performance than the best codes so far for small and moderate code length.

The rest of this paper is organized as follows. Section II defines the proposed codes. Section III describes the decoding algorithm for the proposed codes. In Section IV, we investigate the thresholds for the proposed codes transmitted over the binary erasure channels (BEC) by *density evolution* [4], [17]. In Section V, for the BEC and AWGN channels, we compare the decoding performance of the proposed codes and the best known codes for short and moderate code length.

II. CONCATENATION OF NON-BINARY LDPC CODES AND MULTIPLICATIVE REPETITION CODES

We deal with elements of $\text{GF}(2^m)$ as non-binary symbols. For transmitting over the binary input channels, each non-binary symbol in $\text{GF}(2^m)$ needs to be represented by a binary sequence of length m . For each m , we fix a Galois field $\text{GF}(2^m)$ with a primitive element α and its primitive polynomial π . Once a primitive element α of $\text{GF}(2^m)$ is fixed, each symbol is given a m -bit representation [18, pp. 110]. For example, with a primitive element $\alpha \in \text{GF}(2^3)$ such that $\pi(\alpha) = \alpha^3 + \alpha + 1 = 0$, each symbol is represented as $0 = (0, 0, 0)$, $1 = (1, 0, 0)$, $\alpha = (0, 1, 0)$, $\alpha^2 = (0, 0, 1)$, $\alpha^3 = (1, 1, 0)$, $\alpha^4 = (0, 1, 1)$, $\alpha^5 = (1, 1, 1)$ and $\alpha^6 = (1, 0, 1)$.

A non-binary LDPC code C over $\text{GF}(2^m)$ is defined by the null space of a sparse $M \times N$ parity-check matrix $H = \{h_{ij}\}$ defined over $\text{GF}(2^m)$.

$$C = \{x \in \text{GF}(2^m)^N \mid Hx = 0 \in \text{GF}(2^m)^M\}$$

The c -th parity-check equation for $c = 1, \dots, M$ is written as

$$h_{c1}x_1 + \dots + h_{cN}x_N = 0 \in \text{GF}(2^m),$$

where $h_{c1}, \dots, h_{cN} \in \text{GF}(2^m)$ and $x_1, \dots, x_N \in \text{GF}(2^m)$.

Binary LDPC codes are represented by Tanner graphs with variable and check nodes [19, pp. 75]. The non-binary LDPC codes, in this paper, are also represented by bipartite graphs

with variable nodes and check nodes, which are also referred to as Tanner graphs. For a given sparse parity-check matrix $H = \{h_{cv}\}$ over $\text{GF}(2^m)$, the graph is defined as follows. The v -th variable node and c -th check node are connected if $h_{cv} \neq 0$. By $v = 1, \dots, N$ and $c = 1, \dots, M$, we also denote the v -th variable node and c -th check node, respectively.

A non-binary LDPC code with a parity-check matrix over $\text{GF}(2^m)$ is called (d_v, d_c) -regular if all the columns and all the rows of the parity-check matrix have weight d_v and d_c , respectively, or equivalently all the variable and check nodes have degree d_v and d_c , respectively.

Let C_1 be a (2, 3)-regular LDPC code defined over $\text{GF}(2^m)$ of length N symbols or equivalently mN bits and of rate $1/3$. The code C_1 has a $2N/3 \times N$ sparse parity-check matrix H over $\text{GF}(2^m)$. The matrix H has row weight 3 and column weight 2. Fig. 1 shows the Tanner graph of an example C_1 of length $N = 18$ symbols.

By using C_1 as a mother code, we will construct codes C_2, C_3, \dots, C_T of lower rates in the following way. Choose N coefficients r_{N+1}, \dots, r_{2N} uniformly at random from $\text{GF}(2^m) \setminus \{0\}$. The lower-rate code C_2 is constructed as follows.

$$C_2 = \{(x_1, \dots, x_{2N}) \mid x_{N+v} = r_{N+v}x_v, \text{ for } v = 1, \dots, N, (x_1, \dots, x_N) \in C_1\}.$$

Since the resulting code C_2 has code length $2N$ and the same number of codewords as C_1 , then the rate is $1/6$. Fig. 2 shows the Tanner graph of C_2 of length $2N = 36$ symbols. We say that $x_{N+v} = r_{N+v}x_v$ is a *multiplicative repetition* symbol of x_v for $v = 1, \dots, N$. Each variable node of degree one in Fig. 2 represents a multiplicative repetition symbol x_{N+v} for $v = 1, \dots, N$. And each check node of degree two in Fig. 2 represents a parity-check constraint $x_{N+v} + r_{N+v}x_v = 0$ for $v = 1, \dots, N$.

For $T \geq 3$, in a recursive fashion, by choosing N coefficients $r_{(T-1)N+1}, \dots, r_{TN}$ randomly chosen from $\text{GF}(2^m) \setminus \{0\}$, the further low-rate code C_T is constructed from C_{T-1} as follows.

$$C_T = \{(x_1, \dots, x_{TN}) \mid x_{(T-1)N+v} = r_{(T-1)N+v}x_v, \text{ for } v = 1, \dots, N, (x_1, \dots, x_{(T-1)N}) \in C_{T-1}\}.$$

The code C_T has length TN and rate $1/(3T)$. Fig. 3 shows the Tanner graph of C_3 of $3N = 54$ symbol code length. Fig. 4 shows the block diagram of the encoding of C_3 . We refer to T as *the repetition parameter*.

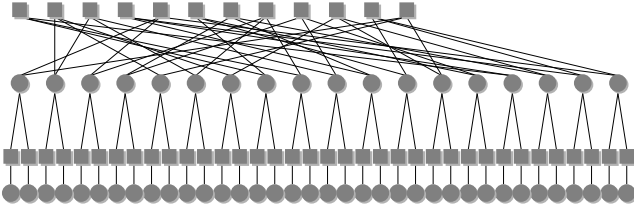


Fig. 3. An example of C_3 . A non-binary (2,3)-regular LDPC code over $\text{GF}(2^m)$ concatenated with one inner multiplicative repetition codes of length 3. The code length is 54 symbols or equivalently $54m$ bits. The rate is $1/9$.

Concatenating a binary code with repetition codes is known as the worst coding scheme. Indeed, repeating a binary code just doubles the number of channel use without any improvement of the curve of the decoding error rate v.s. E_b/N_0 . Note that the proposed code C_T are not generated by simple repetitions of the mother code but the random multiplicative repetitions of non-binary symbols. Since the coefficient $r_{N+v}, \dots, r_{(T-1)N+v} \in \text{GF}(2^m) \setminus \{0\}$ is randomly chosen, the multiplicative repetition $x_v \mapsto (x_v, r_{N+v}x_v, \dots, r_{(T-1)N+v}x_v)$ can be viewed as a random code of length mT bits. In other words, the proposed codes can be viewed as non-binary LDPC codes over $\text{GF}(2^m)$ serially concatenated with N random binary codes of length mT . Intuitively, this explains why multiplicative repetition works better than simple repetition.

The construction of the proposed codes may remind some readers of Justesen codes [20]. Note that the proposed construction chooses the multiplicative coefficients uniformly at random. Note also that since the minimum distance of C_1 is at most $O(\log(N))$ [15], the C_T code has minimum distance is at most $O(T \log(N))$.

Due to the repetition of symbols, the encoder are inherently rate-compatible.

III. DECODING SCHEME

The BP decoder for non-binary LDPC codes [21] exchanges probability vectors of length 2^m , called *messages*, between variable nodes and check nodes, at each iteration round $\ell \geq 0$. The proposed codes C_T for $T \geq 2$ also can be decoded by the BP decoding algorithm on the Tanner graphs of C_T . In this section, instead of the immediate use of the BP decoding on the Tanner graph of C_T , we propose a decoding algorithm which uses only the Tanner graph of C_1 for decoding C_T for $T \geq 2$.

The variable nodes of degree one in Fig. 2 and Fig. 3 represent multiplicative repetition symbols of C_2 and C_3 , respectively. If the BP decoding algorithm is immediately applied to the proposed codes, all the variable nodes and check nodes, including the variable nodes of those multiplicative repetition symbols, are activated, i.e. exchange the messages. However, the messages reaching the variable nodes of degree one do not change messages that are sent back from the nodes. Therefore, the decoder does not need to pass the messages all the way to those variable nodes of degree 1 and their adjacent check nodes of degree 2. Consequently, after the

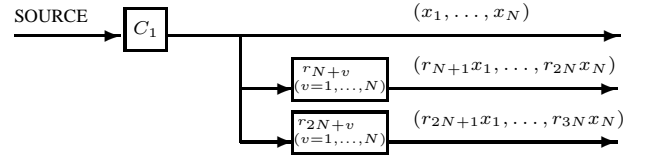


Fig. 4. The block diagram of the encoder of C_3 . First, source of $N/3$ symbols in $\text{GF}(2^m)$ are encoded with a (2,3)-regular LDPC code C_1 over $\text{GF}(2^m)$. Next, each symbol in the codeword x_v , for $v = 1, \dots, N$, is randomly multiplied by r_{N+v} and r_{2N+v} from $\text{GF}(2^m) \setminus \{0\}$ to generate x_{N+v} and x_{2N+v} .

variable nodes of degree 1 pass the initial messages to the upper part of the graph, the decoder uses only the upper part of the graph, i.e. C_1 .

The computations of check nodes are more complex than those of variable nodes. As posed in the Problem 1 in Section I, the number M of the check nodes gets higher as R decreases. In general, LDPC codes of information length K and rate R have $K(1-R)/R$ check nodes. In our setting, we have $K = N/3$ information symbols. The number of check nodes in the proposed code C_T for $T \geq 2$ is also given by $K(1-R)/R$. However, $(T-1)N$ check nodes of degree 2 adjacent to the $(T-1)N$ variable nodes of degree 1 do not need to participate in the BP decoding iterations. The only $2N/3$ active check nodes in the mother code C_1 participate in the BP decoding algorithm for decoding C_T for $T \geq 2$. Note that the number of active check nodes $2N/3$ remains unchanged for any $T \geq 1$. This is highly preferable property for low-rate LDPC codes, which relieves the Problem 1. The Problem 2 is also relieved, since the maximum degree of check nodes in the mother code C_1 is as small as 3.

The BP decoding involves mainly 4 parts, i.e. the initialization, the check to variable computation, the variable to check computation, and the tentative decision parts. For $v = 1, \dots, NT$, let X_v be the random variables with realizations x_v . Let Y_v be the random variables with realizations y_v which is received value from the channel $\Pr(Y_v|X_v)$ and the probability of transmitted symbol $\Pr(X_v)$ is assumed to be uniform.

We assume the decoder knows the channel transition probability

$$\Pr(X_v = x|Y_v = y_v), v = 1, \dots, NT \quad (1)$$

for $x \in \text{GF}(2^m)$. When the transmissions take place over the memoryless binary-input output-symmetric channels, we can rewrite (1) as

$$\Pr(X_v = x|Y_v = y_v) = \prod_{i=1}^m \Pr(X_{v,i} = x_i|Y_{v,i} = y_{v,i}),$$

where $(x_1, \dots, x_m) \in \text{GF}(2)^m$ is the binary representation of $x \in \text{GF}(2^m)$ and $X_{v,i}$ is the random variable of the transmitted bit, and the corresponding channel output $y_{v,i}$ and its random variable $Y_{v,i}$.

A. Decoding Algorithm

initialization :

For each variable node v in C_1 for $v = 1, \dots, N$, compute $p_v^{(0)}(x)$ as follows.

$$p_v^{(0)}(x) = \xi \Pr(X_v = x | Y_v = y_v) \prod_{t=1}^{T-1} \Pr(X_{tN+v} = r_{tN+v} x | Y_{tN+v} = y_{tN+v}), \quad (2)$$

for $x \in \text{GF}(2^m)$, where ξ is the normalization factor so that $\sum_{x \in \text{GF}(2^m)} p_v^{(0)}(x) = 1$. Each variable node $v = 1, \dots, N$ in C_1 sends the initial message $p_{vc}^{(0)} = p_v^{(0)} \in \mathbb{R}^{2^m}$ to each adjacent check node c . Set the iteration round as $\ell := 0$.

check to variable :

For each check node $c = 1, \dots, M$ in C_1 , let ∂c be the set of the adjacent variable nodes of c . It holds that $\#\partial c = 3$, since the mother code C_1 is $(2, 3)$ -regular. Each c has 3 incoming messages $p_{vc}^{(\ell)}$ for $v \in \partial c$ from the 3 adjacent variable nodes. The check node c sends the following message $p_{cv}^{(\ell+1)} \in \mathbb{R}^{2^m}$ to each adjacent variable node $v \in \partial c$.

$$\begin{aligned} \tilde{p}_{vc}^{(\ell)}(x) &= p_{vc}^{(\ell)}(h_{cv}^{-1}x) \text{ for } x \in \text{GF}(2^m), \\ \tilde{p}_{cv}^{(\ell+1)} &= \otimes_{v' \in \partial c \setminus \{v\}} \tilde{p}_{v'c}^{(\ell)}, \\ p_{cv}^{(\ell+1)}(x) &= \tilde{p}_{cv}^{(\ell+1)}(h_{cv}x) \text{ for } x \in \text{GF}(2^m). \end{aligned}$$

where $p_1 \otimes p_2 \in \mathbb{R}^{2^m}$ is a convolution of $p_1 \in \mathbb{R}^{2^m}$ and $p_2 \in \mathbb{R}^{2^m}$. To be precise,

$$(p_1 \otimes p_2)(x) = \sum_{\substack{y, z \in \text{GF}(2^m) \\ x=y+z}} p_1(y)p_2(z) \text{ for } x \in \text{GF}(2^m).$$

The convolution seems the most complex part of the decoding algorithm. Indeed, the convolutions are efficiently calculated via FFT and IFFT [22], [17]. Increment the iteration round as $\ell := \ell + 1$.

variable to check :

Each variable node $v = 1, \dots, N$ in C_1 has two adjacent check nodes since the mother code C_1 is $(2, 3)$ -regular. Let c and c' be the two adjacent check nodes of v . The message $p_{vc}^{(\ell)} \in \mathbb{R}^{2^m}$ sent from v to c is given by

$$p_{vc}^{(\ell)}(x) = \xi p_v^{(0)}(x) p_{c'v}^{(\ell)}(x) \text{ for } x \in \text{GF}(2^m),$$

where ξ is the normalization factor so that $\sum_{x \in \text{GF}(2^m)} p_{vc}^{(\ell)}(x) = 1$.

tentative decision :

For each $v = 1, \dots, N$, the tentatively estimated v -th transmitted symbol is given as

$$\hat{x}_v^{(\ell)} = \underset{x \in \text{GF}(2^m)}{\text{argmax}} p_v^{(0)}(x) p_{cv}^{(\ell)}(x) p_{c'v}^{(\ell)}(x),$$

where c and c' are the two adjacent check nodes of v . If $\hat{\mathbf{x}}^{(\ell)} := (\hat{x}_1^{(\ell)}, \dots, \hat{x}_N^{(\ell)})$ forms a codeword of C_1 , in other words, $\hat{\mathbf{x}}^{(\ell)}$ satisfies every parity-check equations

$$\sum_{v \in \partial c} h_{cv} \hat{x}_v^{(\ell)} = 0 \in \text{GF}(2^m)$$

for all $c = 1, \dots, M$, the decoder outputs $\hat{\mathbf{x}}^{(\ell)}$ as the estimated codeword. Otherwise repeat the latter 3 decoding steps. If the iteration round ℓ reaches a pre-determined number, the decoder outputs FAIL.

The decoder is inherently rate-compatible. Indeed, for decoding the different C_T of rate $1/(3T)$ for $T = 1, 2, \dots$, the decoder only needs the Tanner graph of the mother code C_1 .

IV. ERASURE CHANNEL ANALYSIS

In the binary case, we can predict the asymptotic decoding performance of LDPC codes transmitted over the general memoryless binary-input output-symmetric channels in the large code length limit by *density evolution* [4]. Density evolution also can be used to analyze non-binary LDPC codes [23], [24]. However, for large field size, it becomes computationally intensive and tractable only for the BEC.

Rathi and Urbanke developed the density evolution which enables the prediction of the decoding performance of the non-binary LDPC codes over the BEC in the limit of large code length. For a given code ensemble, density evolution gives the maximum channel erasure probability at which the decoding erasure probability, averaged over all the LDPC codes in the ensemble goes to zero. The maximum channel erasure probability given by the density evolution is referred to as *the threshold*.

It is shown in [17] that for the transmissions over the BEC with non-binary LDPC codes defined over $\text{GF}(2^m)$, the decoding results depend on the binary representation, i.e. the primitive element. In other words, two isomorphic fields do not, in general, yield the identical decoding results. Rathi and Urbanke also observed that the difference of the threshold is of the order of 10^{-4} for the different fields. The density evolution [17] is developed for the non-binary LDPC code ensembles with parity-check matrices defined over the general linear group $\text{GL}(\text{GF}(2), m)$. In this section, we will use the density evolution to evaluate the thresholds of non-binary LDPC codes defined over $\text{GF}(2^m)$. This is a fair approximation, since in [17], it is reported that the threshold for the code ensemble with parity-check matrices defined over $\text{GF}(2^m)$ and $\text{GL}(\text{GF}(2), m)$ have almost the same thresholds within the order of 10^{-4} .

When the transmission takes place over the BEC and all-zero codeword is assumed to be sent, the messages, described by probability vectors $(p(x))_{x \in \text{GF}(2^m)}$ of length 2^m in general, can be reduced to linear subspaces [17] of $\text{GF}(2)^m$. To be precise, for each message in the BP decoding algorithm, a subset of $\text{GF}(2)^m$

$$\{\mathbf{x} \in \text{GF}(2)^m \mid p(\mathbf{x}) \neq 0\},$$

forms a linear subspace of $\text{GF}(2)^m$, where \mathbf{x} is the binary representation of $x \in \text{GF}(2^m)$.

Define $P^{(\ell)} = (P_0^{(\ell)}, \dots, P_m^{(\ell)})$ and $Q^{(\ell)} = (Q_0^{(\ell)}, \dots, Q_m^{(\ell)})$ as the probability vectors of length $m+1$ such that $P_i^{(\ell)}$ (resp. $Q_i^{(\ell)}$) is the probability that a message sent from variable (resp. check) nodes has dimension i at the ℓ -th iteration round of the BP decoding algorithm. The

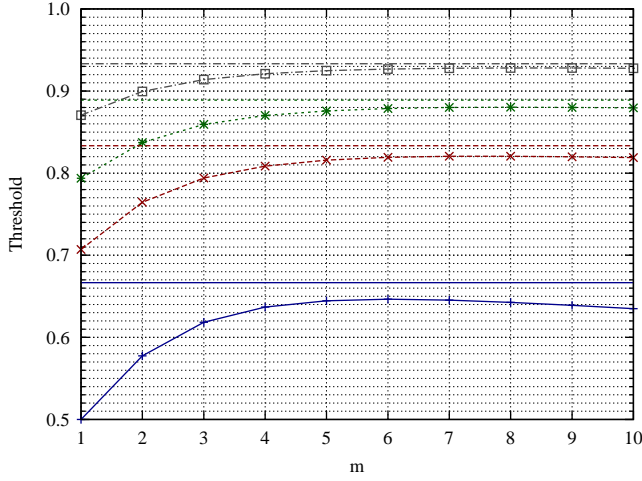


Fig. 5. Thresholds ϵ^* of C_T over $\text{GF}(2^m)$ for the BEC and $T=1,2,3$ and 5 from below. The rate is $1/(3T)$. The straight lines show the Shannon limits $1 - 1/(3T)$.

density evolution gives us the update equations of $P^{(\ell)}$ and $Q^{(\ell)}$ for $\ell \geq 0$.

Rathi and Urbanke[17] developed the density evolution for the BEC that tracks probability mass functions of the dimension of the linear subspaces. For $\ell \geq 0$, the density evolution tracks the probability vectors $P^{(\ell)}$ and $Q^{(\ell)}$ which are referred to as *densities*. The initial messages in (2) can be seen as the intersection of T subspaces of the messages received as the channel outputs. The density of the initial messages is given by $P^{(0)}$ as follows,

$$P^{(0)} = \overbrace{E \boxtimes \dots \boxtimes E}^{T \text{ times}},$$

$$E := (E_0, \dots, E_m),$$

$$E_i := \binom{m}{i} \epsilon^i (1 - \epsilon)^{m-i},$$

where ϵ is the channel erasure probability of the BEC. The operator \boxtimes is defined as follows.

$$[P \boxtimes Q]_k = \sum_{i=k}^m \sum_{j=k}^{k+m-i} C_{\boxtimes}(m, k, i, j) P_i Q_j,$$

$$C_{\boxtimes}(m, k, i, j) := 2^{(i-k)(j-k)} \frac{\binom{i}{k} \binom{m-i}{j-k}}{\binom{m}{j}},$$

where $\binom{m}{k} = \prod_{l=0}^{k-1} \frac{2^m - 2^l}{2^k - 2^l}$ is a 2-Gaussian binomial.

Since the mother code is (2,3)-regular, the update equations of density evolution is given by

$$Q^{(\ell+1)} = P^{(\ell)} \boxtimes P^{(\ell)},$$

$$P^{(\ell+1)} = P^{(0)} \boxtimes Q^{(\ell+1)},$$

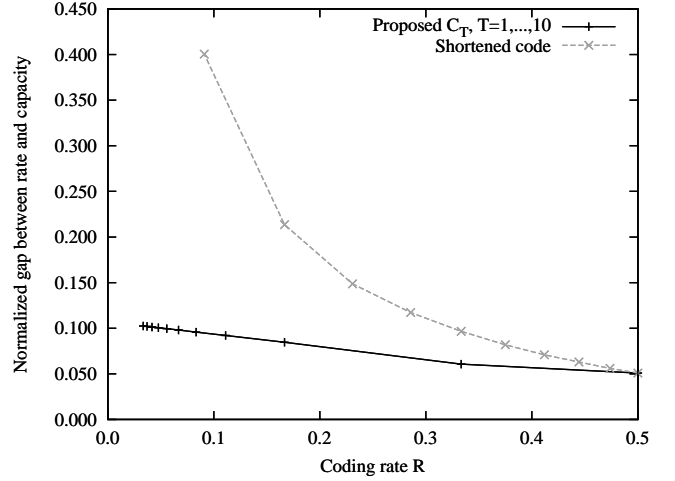


Fig. 6. The asymptotic decoding performance over the BEC of the proposed codes and the best known low-rate codes. One curve corresponds to the proposed code C_T over $\text{GF}(2^6)$ of coding rates $R = 1/(3T)$ with repetition parameter $T = 1, \dots, 10$. The punctured C_1 of rate $1/2$ is also plotted. The other curve corresponds to the bit-wise shortened non-binary LDPC code over $\text{GF}(2^6)$ proposed by Klinc et al. [25, Fig. 1]. The vertical axis indicates $(1 - \epsilon^* - R)/R$ which is the normalized gap between the capacity $1 - \epsilon^*$ and the rate R , where ϵ^* is the threshold.

where the operator \boxtimes is defined as follows.

$$[P \boxtimes Q]_k = \sum_{i=0}^k \sum_{j=k-i}^k C_{\boxtimes}(m, k, i, j) P_i Q_j,$$

$$C_{\boxtimes}(m, k, i, j) := 2^{(k-i)(k-j)} \frac{\binom{m-i}{m-k} \binom{i}{k-j}}{\binom{m}{m-j}}.$$

Since the messages of dimension 0 corresponds to the successful decoding, the threshold is defined as follows.

$$\epsilon^* := \sup_{\epsilon \in [0,1]} \{ \epsilon \in [0,1] \mid \lim_{\ell \rightarrow \infty} P_0^{(\ell)} = 1 \}.$$

In the large code length limit, if $\epsilon < \epsilon^*$ the reliable transmissions are possible with the proposed C_T .

Fig. 5 draws the thresholds of C_T defined with parity-check matrices over $\text{GL}_m(\text{GF}(2))$ for repetition parameter $T = 1, \dots, 5$ and $m = 1, \dots, 10$. The threshold $\epsilon^* = 1/\sqrt[3]{2}$ for the binary case $m = 1$ is decided by the stability condition [19]. It can be seen that the thresholds are not monotonic with respect to m . For repetition parameter $T = 1$, i.e., the mother code has the maximal threshold at $m = 6$. For $T > 2$, the maximal threshold is attained around at $m = 8$.

Fig. 6 compares the proposed codes and the best existing low-rate LDPC codes respect to the thresholds for the BEC. It can be seen that the proposed codes have better thresholds especially for lower rates.

V. NUMERICAL RESULTS

In this section, we give some numerical results of the proposed codes. Fig. 7 shows the decoding performance of the proposed code C_2 whose mother code is a (2,4)-regular non-binary LDPC code defined over $\text{GF}(2^8)$. The transmission

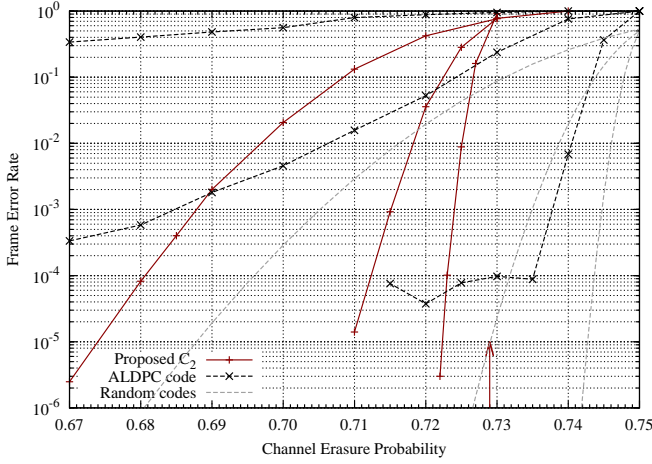


Fig. 7. The solid curve shows the decoding performance of the proposed code C_2 whose mother code is a $(2, 4)$ -regular non-binary LDPC code defined over $\text{GF}(2^8)$. The coding rate is $1/4$. The transmission takes place over the BEC. The arrow indicates the threshold 0.72898 of C_2 . The code length is of length 1024, 8192 and 65536. For comparison, the decoding performance of accumulated LDPC (ALDPC) codes [26, Fig. 15] is shown. It is known that the ALDPC codes achieve the capacity of the BEC in the limit of large code length and exhibit good decoding performance with finite code length. The frame error rate of corresponding random codes of rate $1/4$ under maximum-likelihood decoding are calculated by [27, Eq. (3.2)]. It can be seen that the proposed codes exhibit better decoding performance than the ALDPC codes with code length up to 8192. The error floors of the proposed codes can not be observed down to FER 10^{-5} while the ALDPC codes have high error floors even with code length as long as 65536 bits.

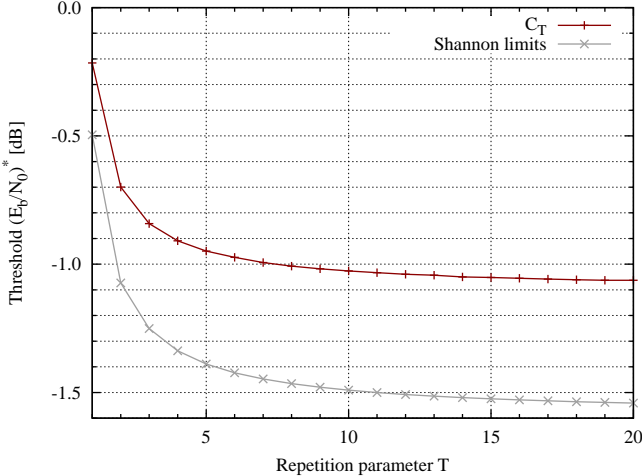


Fig. 8. The thresholds for the AWGN channels of the proposed codes C_T of rate $1/(3T)$ for $T = 1, \dots, 20$. The codes are defined over $\text{GF}(2^8)$.

takes place over the BEC. The compared accumulated LDPC (ALDPC) codes are designed to achieve the capacity in the limit of large code length. It can be seen that the proposed codes exhibit better decoding performance than the ALDPC codes with code length up to 8192. The error floors of the proposed codes can not be observed down to frame error rate 10^{-5} while the ALDPC codes have high error floors even with code length as long as 65536 bits.

Fig. 8 shows the thresholds of the proposed codes C_T of rate $1/(3T)$ for $T = 1, \dots, 20$. The codes are defined over $\text{GF}(2^8)$. The threshold values are calculated by the

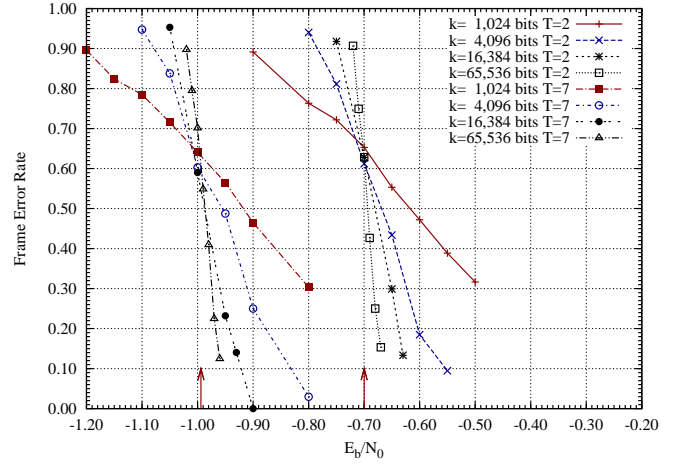


Fig. 9. Frame error rate versus parameter for the proposed codes C_2 and C_7 over $\text{GF}(2^8)$ transmitting over the AWGN channel. The rates of C_2 and C_7 are $1/6$ and $1/21$, respectively. The information length are set to 1024, 4096, 16384, and 65536. The arrows indicate the corresponding threshold values. Observe how the curves move closer to these threshold values for increasing codeword lengths.

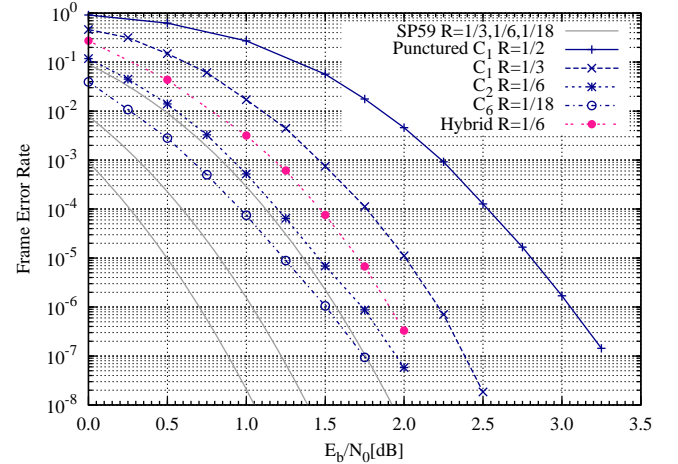


Fig. 10. The frame error rate of the proposed codes C_T for $T = 1, 2, 6$ and hybrid non-binary LDPC codes. It also shows the performance of rate half punctured mother code C_1 . All these codes have 192 information bits. The curves labeled SP59 are the corresponding Shannon's 1959 sphere-packing bound [28], [29], [30] for rate $1/3$, $1/6$ and $1/18$.

Monte Carlo simulation method. The method was originally suggested in [31, p. 22] and an efficient calculation was developed in [32, Section VII]. It can be observed that the proposed codes leave a gap to the ultimate Shannon limit $E_b/N_0 = \log_{10}(\ln(2)) \approx -1.59$ [dB] [8] even in the limit of large repetition parameter T . Fig. 9 depicts the simulation results for the AWGN channels of C_2 and C_7 of very long code length. We observe the convergence to a sharp threshold effect at the predicted threshold values as the information length k increases.

We demonstrate the decoding performance of the short and moderate-length proposed codes C_T for $T = 1, 2, 3, 4, 6$ over the binary-input AWGN channels. The mother code C_1 is constructed by the optimization method in [15]. The

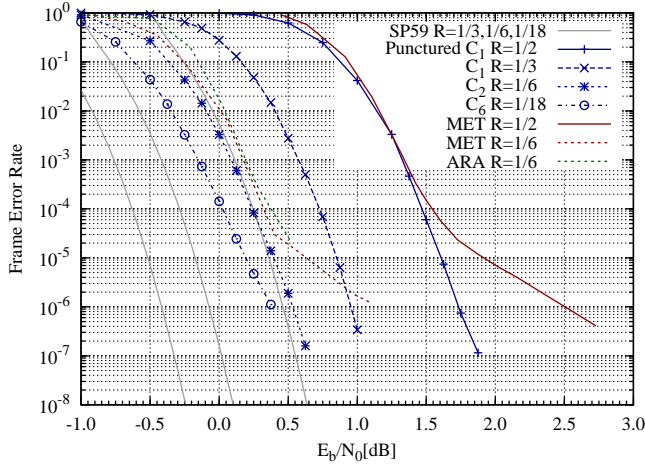


Fig. 11. The frame error rate of the proposed codes C_T for $T = 1, 2, 6$, multi-edge type (MET) LDPC code of rate 1/2 [5] and 1/6, and accumulate repeat accumulate (ARA) code [6] of rate 1/6. All these codes have 1024 information bits except that the MET LDPC code of rate 1/2 has 1280 information bits. It also shows the performance of rate half punctured mother code C_1 . The curves labeled SP59 are the corresponding Shannon's 1959 sphere-packing bounds for rate 1/3, 1/6 and 1/18.

coefficients r_{N+1}, \dots, r_{TN} are chosen uniformly at random from $\text{GF}(2^m) \setminus \{0, 1\}$, where $1 \in \text{GF}(2^m)$ is the multiplicative identity. We fix $m = 8$ for its good performance and the computer-friendly representation of byte.

Fig. 10 shows the decoding performance of C_T for $T = 1, 2, 3, 6$ of rates $1/(3T)$. It also shows a hybrid non-binary LDPC code [16] of rate 1/6 and punctured C_1 of rate 1/2. All these codes have 192 information bits. The proposed code C_2 outperforms the hybrid non-binary LDPC code which is the best code so far for that rate and code length. The code C_3 of rate 1/9 has about 0.5 [dB] coding gain from C_2 of rate 1/6. As we show on these curves, the proposed construction, although simple, allows to design codes with very low rates without large loss of gap to the Shannon limits.

The same property can be seen for the proposed codes with larger information bits. Fig. 11 shows the decoding performance of C_T for $T = 1, 2, 3, 6$, the binary multi-edge type LDPC code of rate 1/2 and 1/6, and the binary ARA code [6] of rate 1/6. All these codes have 1024 information bits except that the MET LDPC code of rate 1/2 has 1280 information bits. It also shows the performance of a punctured mother code C_1 of rate 1/2. Among the codes of rate 1/6, the proposed code C_2 has the best performance both at water-fall and error-floor regions.

As posed in Problem 3, conventional low-rate codes required large code length to exploit the potential performance. It can be seen that the proposed codes exhibit better decoding performance both at small and moderate code length.

VI. CONCLUSIONS

We propose non-binary LDPC codes concatenated with inner multiplicative repetition codes. The performance of the proposed codes exceeds the hybrid non-binary codes, multi-edge type LDPC codes and ARA codes both at the water-fall

and error-floor regions. The encoder and decoder are inherently rate-compatible, and especially the decoder complexity is almost the same as the mother code.

ACKNOWLEDGMENTS

The authors are grateful to T. Richardson for providing the data of the multi-edge type LDPC code of rate 1/6 in Fig. 11. The authors would like to thank anonymous reviewers of ISIT2010 and Transactions on Information Theory, and I. Sason for their suggestions and comments. K. K. wishes to thank T. Uyematsu for valuable comments.

REFERENCES

- [1] K. Kasai, D. Declercq, C. Poulliat, and K. Sakaniwa, "Rate-compatible non-binary LDPC codes concatenated with multiplicative repetition codes," in *Proc. 2010 IEEE Int. Symp. Inf. Theory (ISIT)*, Jun. 2010, pp. 844–848.
- [2] R. G. Gallager, *Low Density Parity Check Codes*. in Research Monograph series, MIT Press, Cambridge, 1963.
- [3] T. Richardson and R. Urbanke, "The capacity of low-density parity-check codes under message-passing decoding," *IEEE Trans. Inf. Theory*, vol. 47, no. 2, pp. 599–618, Feb. 2001.
- [4] T. J. Richardson, M. A. Shokrollahi, and R. L. Urbanke, "Design of capacity-approaching irregular low-density parity-check codes," *IEEE Trans. Inf. Theory*, vol. 47, no. 2, pp. 619–637, Feb. 2001.
- [5] T. Richardson and R. Urbanke, "Multi-edge type LDPC codes," 2003.
- [6] D. Divsalar, S. Dolinar, and C. Jones, "Low-rate LDPC codes with simple protograph structure," in *Proc. 2005 IEEE Int. Symp. Inf. Theory (ISIT)*, Sep. 2005, pp. 1622–1626.
- [7] G. Yue, L. Ping, and X. Wang, "Generalized low-density parity-check codes based on Hadamard constraints," *IEEE Trans. Inf. Theory*, vol. 53, no. 3, pp. 1058–1079, Mar. 2007.
- [8] S. Haykin, *Communication Systems*, 4th ed. John Wiley & Sons, 2001.
- [9] M. Davey and D. MacKay, "Low-density parity check codes over $\text{GF}(q)$," *IEEE Commun. Lett.*, vol. 2, no. 6, pp. 165–167, Jun. 1998.
- [10] W. Chang and J. Cruz, "Nonbinary LDPC codes for 4-kB sectors," *IEEE Trans. Magn.*, vol. 44, no. 11, pp. 3781–3784, Nov. 2008.
- [11] I. Djordjevic and B. Vasic, "Nonbinary LDPC codes for optical communication systems," *Photonics Technology Letters, IEEE*, vol. 17, no. 10, pp. 2224–2226, Oct. 2005.
- [12] B. Zhou, J. Kang, S. Song, S. Lin, K. Abdel-Ghaffar, and M. Xu, "Construction of non-binary quasi-cyclic LDPC codes by arrays and array dispersions," *IEEE Trans. Commun.*, vol. 57, no. 6, pp. 1652–1662, Jun. 2009.
- [13] M. Arabaci, I. Djordjevic, R. Saunders, and R. Marcocchia, "High-rate nonbinary regular quasi-cyclic LDPC codes for optical communications," *Lightwave Technology, Journal of*, vol. 27, no. 23, pp. 5261–5267, Dec. 2009.
- [14] B. Zhou, J. Kang, Y. Tai, S. Lin, and Z. Ding, "High performance non-binary quasi-cyclic LDPC codes on euclidean geometries LDPC codes on euclidean geometries," *IEEE Trans. Commun.*, vol. 57, no. 5, pp. 1298–1311, May 2009.
- [15] C. Poulliat, M. Fossorier, and D. Declercq, "Design of regular $(2, d_c)$ -LDPC codes over $\text{GF}(q)$ using their binary images," *IEEE Trans. Commun.*, vol. 56, no. 10, pp. 1626–1635, Oct. 2008.
- [16] L. Sassatelli, D. Declercq, and C. Poulliat, "Low-rate non-binary hybrid LDPC codes," in *Proc. 5th Int. Symp. on Turbo Codes and Related Topics*, Sep. 2008, pp. 225–230.
- [17] V. Rathi and R. Urbanke, "Density Evolution, Threshold and the Stability Condition for non-binary LDPC Codes," *IEE Proceedings - Communications*, vol. 152, no. 6, pp. 1069–1074, 2005.
- [18] F. J. MacWilliams and N. J. A. Sloane, *The Theory of Error-Correcting Codes*. Amsterdam: Elsevier, 1977.
- [19] T. Richardson and R. Urbanke, *Modern Coding Theory*. Cambridge University Press, Mar. 2008.
- [20] J. Justesen, "Class of constructive asymptotically good algebraic codes," *IEEE Trans. Inf. Theory*, vol. 18, no. 5, pp. 652–656, Sep. 1972.
- [21] M. Davey and D. MacKay, "Low density parity check codes over $\text{GF}(q)$," in *Information Theory Workshop, 1998*, Jun. 1998, pp. 70–71.
- [22] D. Declercq and M. Fossorier, "Decoding algorithms for nonbinary LDPC codes over $\text{GF}(q)$," *IEEE Trans. Commun.*, vol. 55, no. 4, pp. 633–643, Apr. 2007.

- [23] A. Bennatan and D. Burshtein, "On the application of LDPC codes to arbitrary discrete-memoryless channels," *IEEE Trans. Inf. Theory*, vol. 50, no. 3, pp. 417–438, Mar. 2004.
- [24] G. Li, I. Fair, and W. Krzymien, "Density evolution for nonbinary LDPC codes under Gaussian approximation," *IEEE Trans. Inf. Theory*, vol. 55, no. 3, pp. 997–1015, Mar. 2009.
- [25] D. Klinc, J. Ha, and S. McLaughlin, "Optimized puncturing and shortening distributions for nonbinary LDPC codes over the binary erasure channel," in *Proc. 46th Annual Allerton Conf. on Commun., Control and Computing*, Sep. 2008, pp. 1053–1058.
- [26] H. Pfister and I. Sason, "Accumulate repeat accumulate codes: Capacity-achieving ensembles of systematic codes for the erasure channel with bounded complexity," *IEEE Trans. Inf. Theory*, vol. 53, no. 6, pp. 2088–2115, Jun. 2007.
- [27] C. Di, D. Proietti, I. Telatar, T. Richardson, and R. Urbanke, "Finite-length analysis of low-density parity-check codes on the binary erasure channel," *IEEE Trans. Inf. Theory*, vol. 48, no. 6, pp. 1570–1579, Jun. 2002.
- [28] C. E. Shannon, "Capacity of the band-limited Gaussian channel," *Bell System Tech. J.*, vol. 38, pp. 611–656, May 1959.
- [29] A. Valembois and M. Fossorier, "Sphere-packing bounds revisited for moderate block lengths," *IEEE Trans. Inf. Theory*, vol. 50, no. 12, pp. 2998–3014, Dec. 2004.
- [30] G. Wiechman and I. Sason, "An improved sphere-packing bound for finite-length codes over symmetric memoryless channels," *IEEE Trans. Inf. Theory*, vol. 54, no. 5, pp. 1962–1990, May 2008.
- [31] M. Davey, "Error-correction using low-density parity-check codes," Ph.D. dissertation, Univ. Cambridge, Cambridge, U.K., Dec. 1999.
- [32] L. Sassatelli and D. Declercq, "Nonbinary hybrid LDPC codes," *IEEE Trans. Inf. Theory*, vol. 56, no. 10, pp. 5314–5334, Oct. 2010.